Green Chemistry

PAPER

View Article Online
View Journal | View Issue

Cite this: *Green Chem.*, 2026, **28**, 7029

Bioconversion of an untapped lignin monomer into a new pyridine-dicarboxylic acid building block

Pablo Espada-Núñez, [a] Gonzalo Durante-Rodríguez,*[a] Dominic Aboagye,[b] Francesc Medina,[b] Marta Fernández-García,[c] Alexandra Muñoz-Bonilla, [c] Carlos del Cerro-Sánchez *[a] and Eduardo Díaz *[a]

Received 16th January 2026,
Accepted 9th March 2026

DOI: 10.1039/d6gc00315j

rsc.li/greenchem

Bioconversion processes to transform lignin derived compounds into sustainable materials with enhanced properties are capable of integrating lignin valorization and bio-based plastics management in a circular economy model. In this work, synthetic metabolic pathways were designed and implemented into *Pseudomonas putida* KT2440 to efficiently transform the untapped lignin derived monomer homovanillic acid (HVA) into 5-(carboxymethyl)-pyridine-2-carboxylic acid (2,5-CPDCA), a yet unexplored pyridine dicarboxylic acid that can act as a terephthalate analog for the synthesis of new polymers. *O*-Demethylation was the main bottleneck in HVA bioconversion, and it was addressed by engineering an optimized *P. putida* biocatalyst expressing a heterologous 5-aminolevulinic acid synthase that boosts the activity of a heme-dependent cytochrome P450 HVA demethylase. High bioconversion yields were achieved under resting cell conditions using real depolymerized lignin samples. The synthesis and characterization of a novel polymer derived from 2,5-CPDCA confirms its potential as a promising sustainable platform chemical.

Green foundation

1. Most lignin valorization strategies focus on aromatics funneled to protocatechuate, catechol, or gallate, yet lignin depolymerization also yields underexplored aromatics such as homovanillic acid (HVA) that generates homoprotocatechuate as the central intermediate. Here, we present a green strategy to convert HVA into a novel building block, 5-(carboxymethyl)-pyridine-2-carboxylic acid (2,5-CPDCA), enabling the synthesis of a new polyester, poly(1,4-butylene 5-(carboxymethyl)pyridine-2-carboxylate) (PBCP).
2. A synthetic pathway engineered in *Pseudomonas putida* KT2440 enabled the conversion of pure or lignin-derived HVA into 2,5-CPDCA using a resting-cell bioprocess. Boosting intracellular 5-aminolevulinic acid increased bioconversion efficiency to 64% by enhancing cytochrome P450 activity. The resulting monomer was used to synthesize and characterize a novel polyester, PBCP.
3. Further work is required to (i) optimize cyclization of the semialdehyde formed after homoprotocatechuate *meta*-cleavage, (ii) scale up the bioprocess and feedstock concentrations to achieve industrial relevance, and (iii) evaluate the potential of the PBCP polymer for developing materials with improved functional and mechanical properties.

Introduction

The transition to a circular economy requires the redesign of waste management strategies, aiming for more sustainable procedures capable of efficiently reincorporating industrial and domestic residues into the production–consumption cycle. Due to its high recalcitrance towards biological and chemo-catalytic degradation, lignin recycling represents a major challenge in plant-based waste management. Lignin accounts for 30% of the organic carbon in the biosphere and 40% of the energy contained in lignocellulose, and is industrially produced in approximated amounts of 150 million tons per year.[1,2] Although lignin represents a massive source of carbon and energy, and an untapped source of platform chemicals that could displace petroleum-based chemicals, it is mainly inefficiently burned as fuel entailing environmental harms.[3–8] On the other hand, plastic production reached 400.3 million tons per year in 2022, with 90% derived from fossil feedstocks, and over 70% of the resulting non-renewable plastic waste ending up discarded or leaked into the environment, posing significant risks to human health

[a]*Department of Biotechnology, Margarita Salas Center for Biological Research, Spanish National Research Council, Ramiro de Maeztu 9, 28040 Madrid, Spain. E-mail: ediaz@cib.csic.es, carlos.delcerro@cib.csic.es, gdurante@cib.csic.es*
[b]*Departament d'Enginyeria Química, Universitat Rovira i Virgili, Av. Països Catalans, 26, 43007 Tarragona, Spain*
[c]*Institute of Polymer Science and Technology, Juan de La Cierva 3, 28006 Madrid, Spain*

and ecosystems.[9] In this context, bioconversion processes capable of transforming lignin into new sustainable plastic materials with enhanced properties represent novel green alternatives within an open-loop upcycling strategy. Indeed, some examples using green biotechnology strategies already showed the possibilities of bacterial biocatalysts to convert heterogeneous lignin-derived aromatic compounds through natural and engineered biological funneling into bioplastics, *e.g.*, polyhydroxyalkanoates,[10–12] and bio-based plastic building blocks such as *cis*,*cis*-muconic acid,[13–17] 4-vinylphenols,[18] adipic acid,[19] vanillic acid,[20,21] 5-carboxyvanillic acid,[22] 2-pyrone-4,6-dicarboxylic acid (PDC),[23–27] β-ketoadipic acid,[28] or pyridine dicarboxylic acids (PDCAs).[23,29–32]To date, most bioconversion strategies focus on funneling lignin-derived compounds into three main central intermediates: protocatechuate, catechol, and gallate.[3–7,33] However, lignin depolymerization yields a broad spectrum of aromatic compounds, some of which are directed toward alternative central intermediates, such as homoprotocatechuic acid, hydroxyquinol, and alkylcatechols,[34–36] that remain underexplored as potential sources of novel building blocks with unique properties.

PDCA isomers, such as lutidinic acid (2,4-PDCA), isocinchomeronic acid (2,5-PDCA), and dipicolinic acid (2,6-PDCA), have gradually been receiving attention in polyester synthesis for their potential applications in packaging and other areas.[37,38] In this work, we present for the first time an efficient and sustainable bioproduction strategy of the unexplored 5-(carboxymethyl)-pyridine-2-carboxylic acid (2,5-CPDCA). 2,5-CPDCA is a structural analog of homoterephthalic acid, a building block previously used for the production of polymers of less crystallinity than those containing terephthalic acid due to the methylene spacer that confers an asymmetric structure to this monomer.[39–41] Moreover, 2,5-CPDCA has been shown to inhibit the enzyme prolyl 4-hydroxylase, suggesting its potential pharmaceutical relevance in the treatment of human fibrosis.[42] Hence, we have implemented a lignin valorization strategy in which 2,5-CPDCA is produced using homovanillic acid (HVA) as a feedstock compound that generates homoprotocatechuic acid (3,4-dihydroxyphenylacetic acid, HPC) as the central intermediate (Fig. 1A). HVA is commonly found in relevant concentrations after different physicochemical Kraft lignin depolymerization processes (*e.g.*, mechanocatalysis and photocatalysis, solvothermal or hydrothermal decomposition in supercritical water, oxidation in aqueous ionic liquid, *etc.*).[43–48] Here, we have metabolically engineered the model bacterium *Pseudomonas putida* KT2440, a non-pathogenic strain extensively used for lignin valorization,[22,23,26,28,31,49] to efficiently convert HVA into 2,5-CPDCA. We have optimized a resting cell-based bioprocess using HVA as well as actual lignin samples as feedstocks. Additionally, we explored the polymerization properties of 2,5-CPDCA, proposing this monomer as a promising building block for the synthesis of plastic materials with novel properties.

Experimental

Chemicals, bacterial strains, plasmids and growth conditions

Most chemicals were purchased from Merck and Sigma-Aldrich unless otherwise stated. 2,5-CPDCA was purchased from BioSynth Ltd. Bacterial strains and plasmids used in this work are detailed in Table 1. *Escherichia coli* was used for cloning procedures and routinely grown in lysogeny broth (LB)[54] at 37 °C

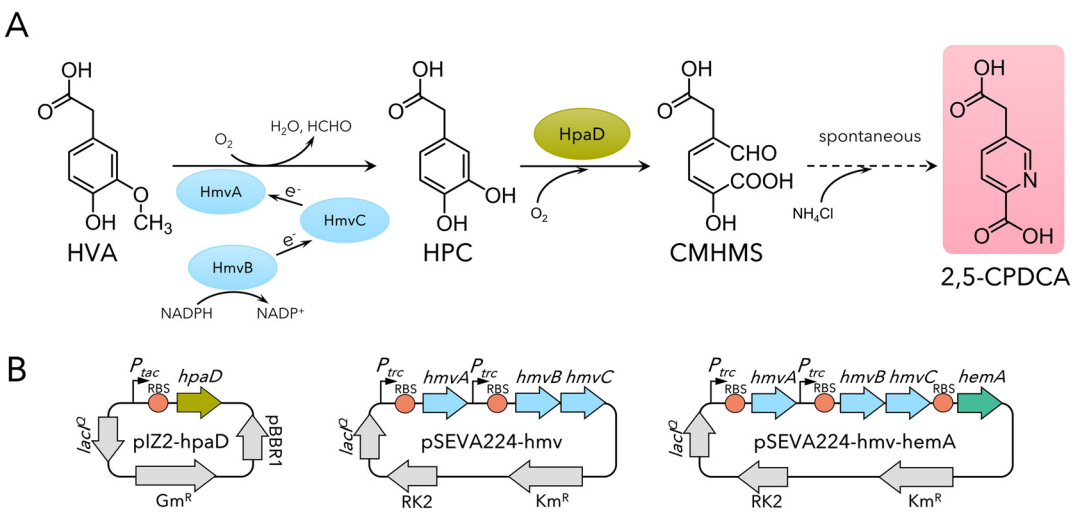

Fig. 1 Bioconversion strategy to generate 2,5-CPDCA in engineered *P. putida* KT2440 strains. (A) Scheme of the reactions introduced into *P. putida* enabling the conversion of HVA into 2,5-CPDCA. Compounds abbreviations: HVA, homovanillic acid; HPC, homoprotocatechuic acid; CMHMS, 5-carboxymethyl-2-hydroxymuconic semialdehyde; 2,5-CPDCA, 5-(carboxymethyl)-pyridine-2-carboxylic acid. Enzyme abbreviations: HpaD, homoprotocatechuate 2,3-dioxygenase; HmvA, homovanillic acid demethylase, P450 subunit; HmvB, ferredoxin NADPH reductase subunit; HmvC, flavodoxin subunit. (B) Schematic representation of the most relevant plasmids used in this work. Colored (non-grey) arrows represent codon-optimized genes, and orange circles represent synthetic ribosome binding sites (RBSs). Maintained native RBS between *hmvB* and *hmvC* is not represented. The P_{tac} and P_{trc} promoters used to express genes of interest are represented with black bent arrows. Regulators ($lacI^q$), origins of replication (pBBR1 and RK2), and antibiotic resistance genes (Gm^R and Km^R) are represented with gray arrows.

Table 1 Bacterial strains and plasmids used in this study

	Relevant genotype	Reference or source
Bacterial strains		
E. coli K12 DH10B	F′, *mcrA* Δ(*mrr hsdRMS-mcrBC*) φ80d*lac*ΔM15 Δ*lacX74 deoR recA1 araD139* Δ(*ara-leu*)7697 *galU galK* λ *rpsL endA1 nupG*	Life Technologies
P. putida KT2440	Wild-type strain	Bagdasarian *et al.*[50]
Plasmids		
pIZ1016	Gm^R, broad-host range expression vector bearing *lacI*^{q} and P_{tac}, and the pBBR1MCS replication origin	Moreno-Ruiz *et al.*[51]
pIZ2	Gm^R, derived from pIZ1016 harboring a different multicloning site	Acedos *et al.*[52]
pIZ2-hpaD	Gm^R, derived from pIZ2 and expressing *hpaD* from *Klebsiella pneumoniae* M5a1 under the *lacI*^{q}/P_{tac} regulatory couple	This work
pSEVA224	Km^R, broad-host range expression vector bearing *lacI*^{q} and P_{trc}, and the RK2 replication origin	Silva-Rocha *et al.*[53]
pSEVA224-hmv	Km^R, derived from pSEVA224 and expressing *hmvA*, *hmvB*, and *hmvC* from *Paenarthrobacter nitroguajacolicus* under the *lacI*^{q}/P_{trc} regulatory couple	This work
pIZ2-hemA	Gm^R, derived from pIZ2 expressing *hemA* from *Rhodobacter capsulatus* under the *lacI*^{q}/P_{tac} regulatory couple	This work
pSEVA224-hmv-hemA	Gm^R, derived from pIZ2-hmv expressing *hmvA*, *hmvB*, and *hmvC* from *Paenarthrobacter nitroguajacolicus* and *hemA* from *Rhodobacter capsulatus*, all genes under the *lacI*^{q}/P_{trc} regulatory couple	This work

with 200 rpm agitation. *P. putida* KT2440 was used for all bioconversion experiments and cultivated in LB or M63 minimal medium (13.6 g L^{-1} KH_2PO_4, 2 g L^{-1} $(NH_4)_2SO_4$, 0.5 mg L^{-1} $FeSO_4 \times 7\ H_2O$, adjusted to pH 7.0 with KOH)[55] at 30 °C and 200 rpm. The M63 minimal medium was supplemented with 0.2% glucose as the carbon source, 1 mM $MgSO_4$, and 1× trace element solution (composition 1000× dissolved in 1 N HCl: 2.78 g L^{-1} $FeSO_4 \times 7H_2O$, 1.98 g L^{-1} $MnCl_2 \times 4H_2O$, 2.81 g L^{-1} $CoSO_4 \times 7H_2O$, 1.47 g L^{-1} $CaCl_2 \times 2H_2O$, 0.17 g L^{-1} $CuCl_2 \times 2H_2O$, 0.29 g L^{-1} $ZnSO_4 \times 7H_2O$).[56] Antibiotics were added when required at the following concentrations: gentamicin (10 μg mL^{-1}) or kanamycin (50 μg mL^{-1}). Induction of gene expression was carried out with 1 mM IPTG when required. Bacterial growth was determined by measuring absorbance at 600 nm (OD_{600}) using a Shimadzu UV-1900i spectrophotometer.

Molecular biology techniques

Standard molecular biology techniques were performed as previously described.[54] DNA fragments were purified from PCR amplification mixtures or agarose gels using a PureLink™ PCR Micro Kit or a Quick Gel Extraction Kit, respectively (Invitrogen). Plasmids were extracted with the High Pure Plasmid Isolation Kit (Roche). Restriction enzymes and T4 DNA ligase (New England Biolabs) were used following the manufacturer's standard protocols. Cloned inserts and/or complete plasmid sequences were confirmed by DNA sequencing in an ABI Prism 377 DNA sequencer or by Oxford Nanopore sequencing at Plasmidsaurus, Inc. *E. coli* transformation was performed using the RbCl method,[54] and *P. putida* was transformed by electroporation (2.5 kV, 25 μF, 200 Ω)[57] using a Gene Pulser/Pulse Controller (Bio-Rad).[54]

Plasmid construction

The genes *hmvABC* from *P. nitroguajacolicus*, also known as CYP1232A24 (WP_091470958), FeRed_1 (WP_091470967), and FldX (WP_091470964), respectively,[58] the *hpaD* gene from *K. pneumoniae*,[59] and the *hemA* gene from *R. capsulatus*[60] were all codon optimized (sequences are listed in Table S1) before being synthesized (GenScript) using pIZ2 and pSEVA224 as backbones to obtain plasmids pSEVA224-hmv, pIZ2-hpaD, and pIZ2-hemA (Fig. 1B and Table 1). Plasmid pSEVA224-hmv-hemA was constructed after digesting pIZ2-hemA with restriction enzymes *Pst*I and *Hin*dIII, and then ligating the *hemA* restriction product into a *Pst*I/*Hin*dIII double-digested pSEVA224-hmv plasmid (Fig. 1B and Table 1).

2,5-CPDCA production coupled to bacterial growth

P. putida KT2440 strains were cultivated in 10 mL of M63 medium with 0.2% glucose as the carbon source in 50 mL flasks. Pre-cultures were grown for 24 h and then used to inoculate (1 : 100 dilution) 20 mL of fresh M63 medium with 0.2% glucose in 100 mL flasks. Cultures were supplemented with 50 mM NH_4Cl and 1 mM HVA. After 3 h, IPTG (1 mM) was added to induce expression of *hpaD* and *hmvABC* genes. Samples were collected over 24 h, measuring bacterial growth by determining OD_{600}, and centrifuged (13 000 rpm for 10 min), and the supernatants were filtered (0.22 μm PES, Sartorius) and stored at −20 °C for further metabolite analyses.

2,5-CPDCA production in resting cell assays

Pre-cultures of *P. putida* KT2440 were grown in 10 mL of LB in 50 mL flasks and then used to inoculate (1 : 100 dilution) 100 mL of LB in 0.5 L flasks. When required, cultures were supplemented with 1 mM $FeSO_4$ and/or 1 mM 5-ALA as indicated. After 3 h, IPTG (1 mM) was added and the cultures were incubated for an additional 21 h. The cells (0.16 ± 0.08 g dry cell weight) were harvested and resuspended in 10 mL of resting cell buffer (20 mM sodium phosphate pH 7.5, 0.2% glucose, 0.1% NH_4Cl). Substrates added included 1 mM HVA, or 10 mL of a 1 : 2 dilution of depolymerized lignin mixture (Table S2) in resting cell buffer. Reactions were carried out in 50 mL flasks at 30 °C and 200 rpm for up to 48 h. Samples were centrifuged and filtered and the supernatants were stored at −20 °C for further metabolite analysis.

Lignin depolymerization

Lignin depolymerization mixtures were generated by mechanocatalytic and photocatalytic methods as previously described.[43] Briefly, 4 g of oven-dried alkaline lignin (L0082, TCI Chemical

Reagent) was suspended in 75 mL of diethyl ether containing 1.5 mmol H_2SO_4 per gram of lignin. The mixture was stirred for 2 h at room temperature. The solvent was evaporated at 40 °C using a rotary evaporator, and the acid-impregnated lignin was stored at 4 °C until further use. The acid-impregnated lignin (2 g) was ball milled in an 80 mL stainless steel jar using five 10 mm stainless steel balls. Milling was conducted at 600 rpm for 60 minutes in four cycles of 15 min milling and 10 min rest. For depolymerization, a weighed amount of pretreated lignin was dispersed in deionized water (*e.g.*, 4.2 g L^{-1}) with 1.5 g L^{-1} TiO_2 (Aeroxide® P25). The mixture was stirred in the dark for 15 minutes to reach adsorption equilibrium. Irradiation was carried out for 60 minutes under UV light (300–400 nm) using a SUNTEST CPS + solar simulator (250 W m^{-2}) at unadjusted pH 8. After the reaction, the mixture was filtered (0.22 μm PTFE), extracted three times with ethyl acetate, and analyzed using GC/MS (for product identification) and GC/FID (for product quantification) as previously detailed.[43] Commercial standards (Sigma-Aldrich) of vanillin, acetovanillone, guaiacol, HVA, and vanillic acid were used for GC calibration.

Metabolite analysis

Metabolite concentrations were determined by HPLC using a 1260 Infinity II system (Agilent) equipped with a ZORBAX Eclipse Plus C18 reverse-phase column (4.6 × 250 mm, 5 μm). UV detection was carried out at 280 nm (for 4-HPA, HVA, and HPC) and 270 nm (for 2,5-CPDCA), using a diode array type of UV/VIS detector (DAD). The mobile phases were solvent A (water with 0.1% trifluoroacetic acid) and solvent B (methanol with 0.1% trifluoroacetic acid). The gradient was: 15%–50% B over 11 min, followed by 50%–15% B for 1 min, and then 15% B for 4 min. The flow rate was 1 mL min^{-1}. Quantification was performed by comparison with commercial standards. 2,5-CPDCA, HVA, and HPC peaks were identified approximately at 3.3, 10.4, and 7.5 min, respectively.

HPLC-MS (high-performance liquid chromatography coupled with mass spectroscopy) analyses were performed using 1260 Infinity II and Infinity Lab LC/MSD XT systems (both from Agilent) and a Poroshell 120 EC-C18 (4.6 × 100 mm, 4 μm, Agilent) reverse phase column. The solvents used for HPLC analyses were water/0.1% formic acid (solvent A) and acetonitrile/0.1% formic acid (solvent B). The applied gradient for analysis was 0–40% of solvent B for 12 min followed by a 3 min column re-equilibration step in which solvent B was restored to 0%. The flow rate was always kept at 1 mL min^{-1}. Chromatograms generated from the samples were compared to commercial standards. The identity of 2,5-CPDCA was confirmed by extracted ion analysis at 182 *m*/*z*, in the positive ion mode, and it was compared with the profile generated by the commercial standard.

Synthesis of the PBCP polymer

Monomers 2,5-CPDCA (1 mmol) and 1,4-butanediol (BD) (1 mmol) were poured into a two-neck round-bottom flask, which was degassed with argon. Then, the catalyst stannous octoate ($Sn(Oct)_2$) was added and the reaction mixture was stirred for 24 h at 180 °C under an argon atmosphere. After that, the mixture was cooled down to room temperature and precipitated in chloroform. The resulting solid was washed several times with chloroform.

Polymer characterization techniques

Proton nuclear magnetic resonance (^{1}H-NMR). The characterization of the polymer was confirmed from ^{1}H NMR spectra at 400 MHz obtained on a Varian Mercury 400 spectrometer using deuterated dimethyl sulfoxide (DMSO-d_6) as the solvent. The value of polymerization degree (n) was calculated using the ratio between the signals of the catalyst and polymer as follows: $n = \dfrac{\left(I_{6,7,b,c,d,e,f,g} - 12 \times \dfrac{I_a}{3}\right)}{4}$ or $n = \dfrac{I_1}{\dfrac{I_a}{3}}$.

Size exclusion chromatography (SEC). The molecular weight was determined by SEC using a Waters HPLC chromatograph equipped with a Waters 2414 refractometer index detector using *N*,*N*-dimethylformamide (DMF) styragel columns. As an eluent, DMF containing 0.1% of LiBr was used at a flow rate of 0.7 mL min^{-1} at 50 °C. The calibration curve was obtained using poly (methyl methacrylate) standards (Polymer Laboratories LTD) ranging from 4.8 × 10^5 to 2990 Da. The samples were dissolved in DMF and filtered through a 0.45 μm Teflon filter before the analysis.

Differential scanning calorimetry (DSC). Thermal characteristics of the polymer were studied by DSC using a TA Q2000 (TA Instruments). The sample was heated from −50 °C to 150 °C at 10 °C min^{-1}, and then a rapid cooling scan to −50 °C was performed. A second heating scan from −50 °C to 150 °C at 10 °C min^{-1} was carried out. Nitrogen purge (50 cm^3 min^{-1}) was applied for the whole experiment.

Thermogravimetric analysis (TGA). The thermal stability was evaluated by thermogravimetric analysis (TGA) using a TGA2 STAR SYSTEM thermal analyzer (Mettler Toledo). The measurements were conducted under dynamic conditions and a nitrogen atmosphere, heating from 30 °C to 600 °C at a heating rate of 10 °C min^{-1}.

Quantification and statistical analysis

The data presented are based on biological replicates ($n \geq 3$). Means and standard deviations were calculated using Microsoft Excel. No additional statistical tests were applied unless otherwise stated.

Results and discussion

Engineering *P. putida* KT2440 recombinant biocatalysts for the bioconversion of HVA into 2,5-CPDCA

HVA is a catabolic intermediate in the papaverine degradation pathway of the Gram-positive bacterium *Paenarthrobacter nitroguajacolicus* strain HG.[58] HVA is demethoxylated to the central intermediate HPC by a cytochrome P450 monooxygenase system composed of three components: CYP1232A24 (a P450 enzyme),

FeRed1 (a ferredoxin-NADPH reductase), and FldX (a flavodoxin), referred to as HmvA, HmvB, and HmvC, respectively, in this work (Fig. 1A).[58] In some bacteria, HPC is subsequently subjected to a *meta*-cleavage reaction catalyzed by homoprotocatechuate 2,3-dioxygenase (HpaD), generating 5-carboxymethyl-2-hydroxymuconic semialdehyde (CMHMS) (Fig. 1A).[61–64] Although CMHMS is further degraded to succinate and pyruvate by downstream enzymes of the hpa pathway, this highly reactive intermediate was also reported to spontaneously cyclize into 2,5-CPDCA in the presence of ammonium (Fig. 1A).[65,66] Based on this, we hypothesized that heterologous expression of the *hmvABC* and *hpaD* genes in a bacterial chassis lacking CMHMS-degrading activity could enable efficient bioconversion of HVA into 2,5-CPDCA in the presence of ammonium. We selected *P. putida* KT2440 as the host (Table 1), as this model strain has been extensively engineered for the conversion of aromatic compounds, including lignin-derived monomers, into PDCAs,[23,31,32] and it notably lacks the native hpa pathway, making it unable to degrade or modify CMHMS.

To engineer a synthetic HVA *O*-demethylation module and an HPC *meta*-cleavage module, we modified the *hmvABC* genes from *P. nitroguajacolicus*[58] and the *hpaD* gene from *Klebsiella pneumoniae* M5a1,[59] respectively, by incorporating synthetic ribosome binding sites and placing them under the control of the $lacI^q/P_{trc}$ or $lacI^q/P_{tac}$ regulatory systems that enabled controlled gene expression upon IPTG addition (Fig. 1B). The resulting plasmids, pSEVA224-hmv and pIZ2-hpaD (Fig. 1B and Table 1), were then introduced into *P. putida* KT2440 cells. The recombinant strain *P. putida* KT2440 (pIZ2-hpaD, pSEVA224-hmv) was initially tested for its ability to produce 2,5-CPDCA when growing in minimal medium with glucose as the carbon source, ammonium, and HVA as the substrate. Unlike the control KT2440 strain carrying the parental pIZ2 and pSEVA224 vectors, the *P. putida* KT2440 (pIZ2-hpaD, pSEVA224-hmv) strain showed HVA consumption and a modest 2,5-CPDCA conversion yield of 9.5 ± 1.1% (mol/mol) after 24 h of growth (Fig. 2A), thereby validating the proposed bioconversion process.

Given that resting cells offer an effective strategy for the production of aromatic compounds,[31,67,68] we evaluated their use for the bioconversion of HVA into 2,5-CPDCA. *P. putida* KT2440 cells harboring either the control plasmids or the expression plasmids pIZ2-hpaD and pSEVA224-hmv were cultivated in LB medium and subsequently resuspended in resting cell buffer supplemented with HVA. Supernatant samples were collected over time to monitor the biotransformation of HVA into 2,5-CPDCA through HPLC-MS analyses (Fig. S1). Resting cells of *P. putida* KT2440 (pIZ2-hpaD, pSEVA224-hmv) exhibited higher HVA consumption than growing cells and achieved a superior 2,5-CPDCA conversion yield, reaching up to 34.6 ± 1.8% (mol/mol) (Fig. 2B). Nevertheless, 2,5-CPDCA production levels remained significantly low. Considering that no HPC accumulation was detected, the *O*-demethylation of HVA by the HmvABC cytochrome P450 system appeared to be the rate-limiting step. In this sense, it has been previously reported that *O*-demethylation is a rate-determining step in the biocatalytic conversion of lignin-derived aromatic compounds.[2,8,69] Based on these results, we conducted further investigations to address this bottleneck.

Enhancing 2,5-CPDCA production from HVA by the external addition of 5-aminolevulinic acid (5-ALA) and iron to the bacterial biocatalyst

Given that cytochrome P450 enzymes require heme as a cofactor, supplementation of bacterial cultures with the heme precursor 5-aminolevulinic acid (5-ALA) and iron has been reported as an effective strategy to boost their enzymatic activity.[70,71] To address the bottleneck in the bioconversion of HVA to 2,5-CPDCA, likely caused by limited activity of the HmvABC cytochrome P450 system, we supplemented the

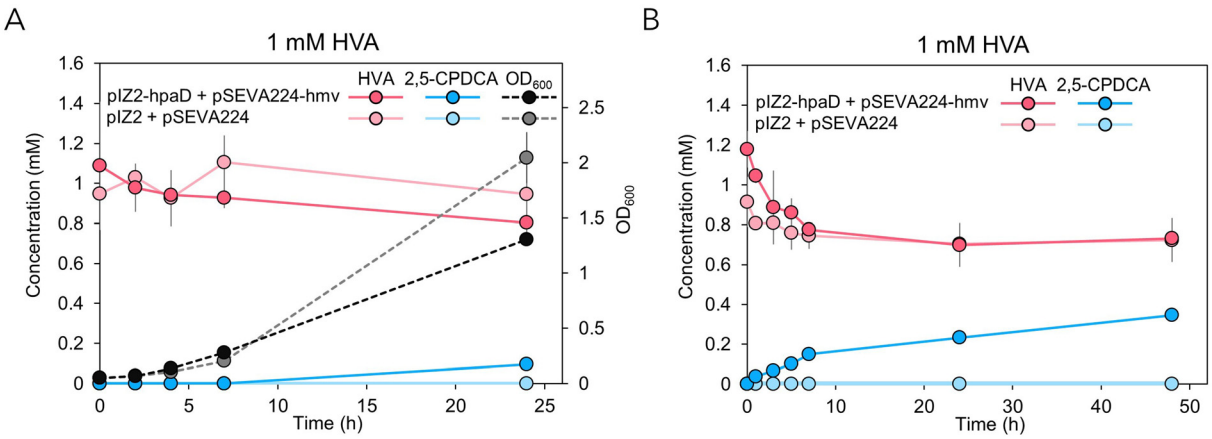

Fig. 2 2,5-CPDCA bioproduction assays from HVA in *P. putida* KT2440 recombinant strains. 2,5-CPDCA production profiles from 1 mM HVA as a substrate when using *P. putida* growing cultures (A) or resting cells (B) are shown. Metabolite concentrations are represented with continuous lines: HVA (red) and 2,5-CPDCA (blue). HPC was not detected under any experimental condition. OD_{600} in growth assays is represented with discontinuous lines (grey). Light colors refer to *P. putida* KT2440 control strains harboring pIZ2 or pSEVA224 empty plasmids. Intense colors refer to *P. putida* KT2440 strains expressing the *hmvABC* and *hpaD* genes (pIZ2-hpaD, pSEVA224-hmv). Error bars represent the standard deviation of the triplicate.

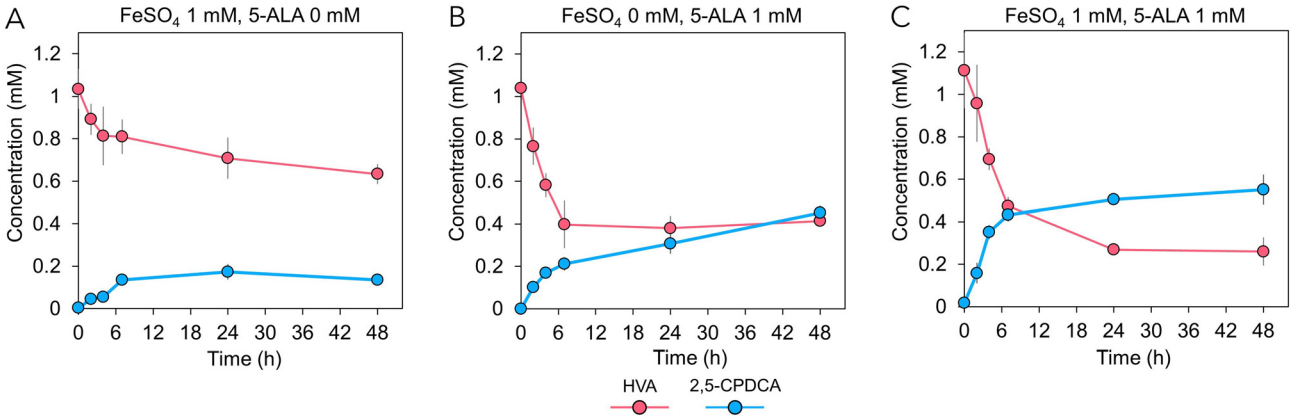

Fig. 3 Effect of $FeSO_4$ and/or 5-ALA in 2,5-CPDCA bioproduction assays. Resting cell assays were performed for 48 h using a *P. putida* KT2440 recombinant strain harboring pIZ2-hpaD and pSEVA224-hmv plasmids, which was cultivated in a medium supplemented with $FeSO_4$ 1 mM (A), 5-ALA 1 mM (B), or $FeSO_4$ 1 mM plus 5-ALA 1 mM (C). No HPC was detected in any of the analyzed samples. Error bars represent the standard deviation of the triplicate.

culture medium used to grow *P. putida* KT2440 (pIZ2-hpaD, pSEVA224-hmv) cells with $FeSO_4$ and/or 5-ALA. These cells were subsequently used in the resting cell assays with HVA as the substrate. The results showed that $FeSO_4$ supplementation alone did not increase the 2,5-CPDCA yield (Fig. 3A), suggesting that intracellular heme availability is the limiting factor for cytochrome P450 activity. Accordingly, supplementation with 5-ALA (heme precursor) significantly enhanced HVA consumption and increased the 2,5-CPDCA yield to up to 45.2 ± 3.4% (mol/mol) (Fig. 3B). Interestingly, when $FeSO_4$ and 5-ALA were simultaneously added to the culture medium, the production rate of 2,5-CPDCA accelerated, the consumption of HVA increased, and the final 2,5-CPDCA conversion yield was enhanced further to up to 55.2 ± 7.1% (mol/mol) after 48 h (Fig. 3C), reaching a production titer of 0.1 g L^{-1}. All these results suggest that the availability of the heme cofactor is essential for efficient HVA demethylation catalyzed by the HmvABC cytochrome P450. As expected, $FeSO_4$ supplementation enhanced HVA consumption and 2,5-CPDCA yield only when sufficient heme cofactor was synthesized. In all cases, the amount of 2,5-CPDCA produced consistently remains lower than the amount of HVA consumed (Fig. 3). Since no HPC intermediate was detected (Fig. 3) and cells tolerate concentrations of 2,5-CPDCA of at least 5 mM (Fig. S2), the spontaneous cyclization of CMHMS may be a critical step that should be targeted for optimization. For example, the effects of ammonium concentration, pH, temperature, and other reaction parameters could be systematically evaluated to further enhance bioconversion efficiency.

Expression of a heterologous 5-aminolevulinic acid synthase in *P. putida* biocatalysts improves the bioconversion of HVA into 2,5-CPDCA

As demonstrated above, the exogenous addition of 5-ALA enhances the bioconversion of HVA into 2,5-CPDCA; however, the high cost of commercially available 5-ALA poses a significant challenge to the economic viability of the process. To overcome this limitation, we pursued an alternative approach focused on boosting endogenous 5-ALA production to avoid reliance on external supplementation. 5-ALA bioproduction in nature can be accomplished through two different pathways, *i.e.*, the C-5 pathway from α-ketoglutarate, and the C-4 pathway from glycine and succinyl-coenzyme A. The C-5 pathway exists in algae, higher plants, and many bacteria including *Escherichia coli* or *P. putida* KT2440. However, the C-4 pathway appears in birds, mammals, yeasts, and purple non-sulfur-photosynthetic bacteria.[72,73] The overexpression of the C-4 pathway enzyme 5-aminolevulinic acid synthase (ALAS) has been reported to increase the efficiency of the heterologous production of a cytochrome P450 in *E. coli*.[60] Following this approach, we used the *hemA* gene encoding an ALAS enzyme from the purple bacterium *Rhodobacter capsulatus*,[74] expecting an increase in the intracellular 5-ALA, and consequently, in the heme group levels, promoting HmvABC activity in *P. putida* (Fig. 4A). A synthetic *P. putida* codon-optimized version of *hemA* was cloned into pSEVA224-hmv, generating plasmid pSEVA224-hmv-hemA, in which the expression of both *hmvABC* and *hemA* can be induced by IPTG (Fig. 1B and Table 1). As anticipated, the strain expressing the *hemA* gene acquired a pronounced red-brown coloration, indicative of substantial heme group accumulation (Fig. 4B), and we did not observe a significant defect in cell growth compared with the strain lacking *hemA* (Fig. S3), suggesting that overexpression of this gene does not cause a metabolic burden on *P. putida*. Subsequently, resting cell assays were carried out using a *P. putida* KT2440 strain co-expressing *hpaD*, *hmvABC*, and *hemA* to evaluate the efficiency of HVA bioconversion into 2,5-CPDCA. The results demonstrated that ALAS expression enhanced the bioconversion process, achieving 2,5-CPDCA conversion yields up to 63.6 ± 6.4% after 48 h (Fig. 4C), with a production titer (0.12 g L^{-1}) that surpasses even the levels achieved with exogenous 5-ALA supplementation. The pro-

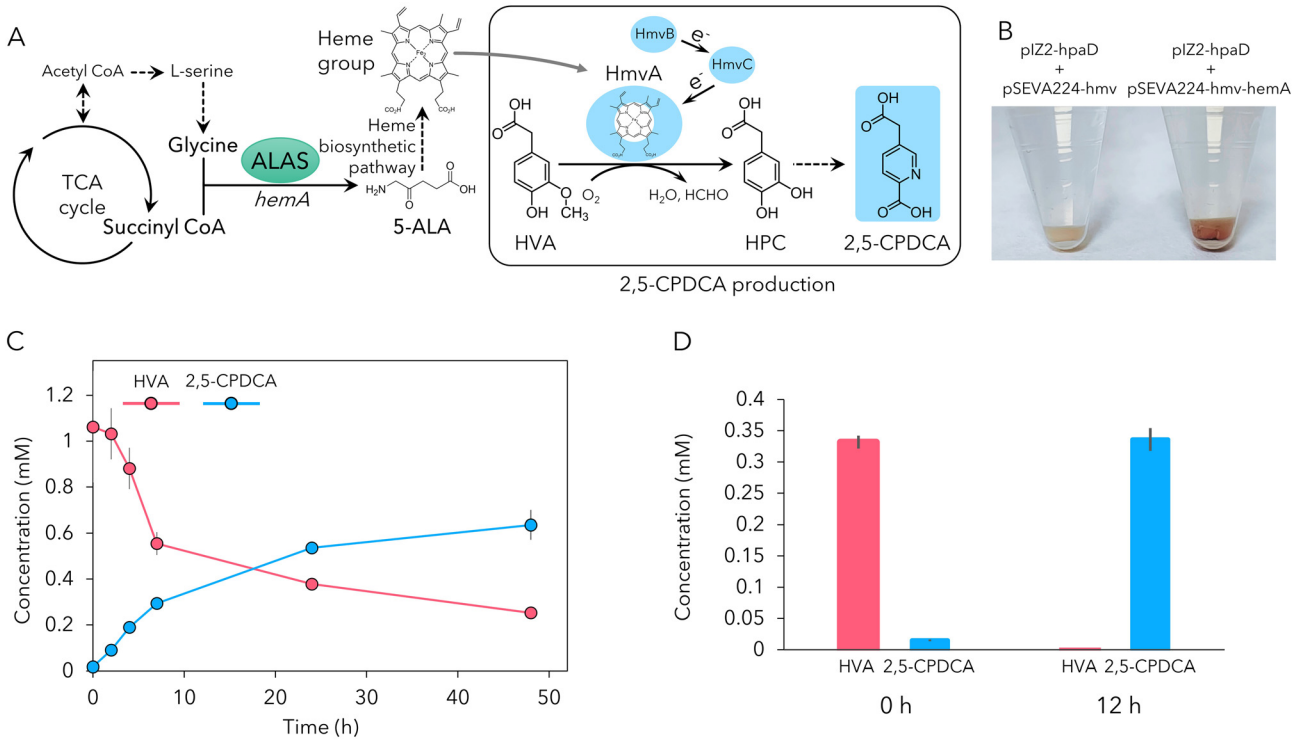

Fig. 4 Bioconversion of HVA into 2,5-CPDCA using *P. putida* KT2440 recombinant strains expressing the *hemA* gene. (A) Schematic representation of the engineered C4 5-ALA biosynthesis pathway and 2,5-CPDCA production in *P. putida*. (B) Photograph of cell pellets of recombinant *P. putida* KT2440 strains harboring the pIZ2-hpaD and pSEVA224-hmv or pSEVA224-hmv-hemA (expressing the *hemA* gene) plasmids after growing for 24 h in M63 minimal media supplemented with $FeSO_4$ 1 mM. (C) HVA consumption and 2,5-CPDCA production profiles during 48 h in resting cells using pure HVA after pre-culturing *P. putida* KT2440 cells harboring plasmids pIZ2-hpaD and pSEVA224-hmv-hemA in a medium supplemented with $FeSO_4$ 1 mM. (D) HVA consumption and 2,5-CPDCA production after 12 h in resting cells using depolymerized alkaline lignin. The *P. putida* KT2440 cells harboring plasmids pIZ2-hpaD and pSEVA224-hmv-hemA were grown in a medium supplemented with $FeSO_4$ 1 mM. Error bars represent the standard deviation of triplicate.

ductivity of 2,5-CPDCA reached 7.6 mg/L h^{-1}. Moreover, our results show for the first time that engineering a recombinant *P. putida* KT2440 strain to express the *hemA* gene constitutes an effective strategy to enhance the activity of a heterologous cytochrome P450, thereby broadening the scope of bioprocesses that can be efficiently implemented in this model bacterium.

Since the results described above were achieved using pure HVA, we further evaluated the performance of the engineered *P. putida* KT2440 strain expressing *hpaD*, *hmvABC*, and *hemA* genes with real depolymerized lignin samples. To this end, alkaline lignin was subjected to a depolymerization protocol combining mechanocatalysis (involving prior acid impregnation followed by ball milling) and photocatalysis using TiO_2.[43] This process yielded a lignin derived mixture enriched in HVA (Table S2). This mixture was directly added to a resting cell solution at a 1 : 2 dilution, resulting in a final HVA concentration of 0.33 mM. The engineered biocatalyst completely consumed the available HVA and after 8 h an almost equimolar amount of 2,5-CPDCA was detected (Fig. 4D), yielding a 2,5-CPDCA production titer of 0.06 g L^{-1}, and a productivity of 7.5 mg/L h^{-1}. Therefore, these results demonstrate that the *P. putida* KT2440 strain carrying plasmids pIZ2-hpaD and pSEVA224-hmv-hemA functions as an efficient biocatalyst for converting HVA into 2,5-CPDCA using pretreated lignin as a renewable feedstock, and they suggest that other aromatic compounds present in the lignin sample do not significantly interfere with HVA bioconversion efficiency.

Characterization of the 2,5-CPDCA-derived polymer (PBCP)

The synthesis of a new polymer, poly(1,4-butylene 5-(carboxymethyl)pyridine-2-carboxylate) or PBCP, was performed in bulk with an equimolecular ratio of 2,5-CPDCA and 1,4-butanediol co-monomers using $Sn(Oct)_2$ at 180 °C. After that, the mixture was precipitated and purified, affording a pale-yellow-orange powder (Fig. 5), yield *ca.* 82%. The success of the synthesis was confirmed by proton NMR, where no acidic proton signal was detected in the spectrum (Fig. 5). At 0.85 ppm, 1.24 ppm, and 1.42 ppm, methyl, methylene and methine signals of the catalyst appear, respectively. On the other hand, between 1.24 and 1.42 ppm, the peaks of inner methylene protons of the butylene monomer appear, while those for the outer methylene protons appear between 4.0 and 4.73 ppm. The two protons of $-CH_2-COO-$ moieties near the pyridine group are observed at 3.82 ppm, while the methine protons of the pyridine ring appear between 7.65 and 8.98 ppm.

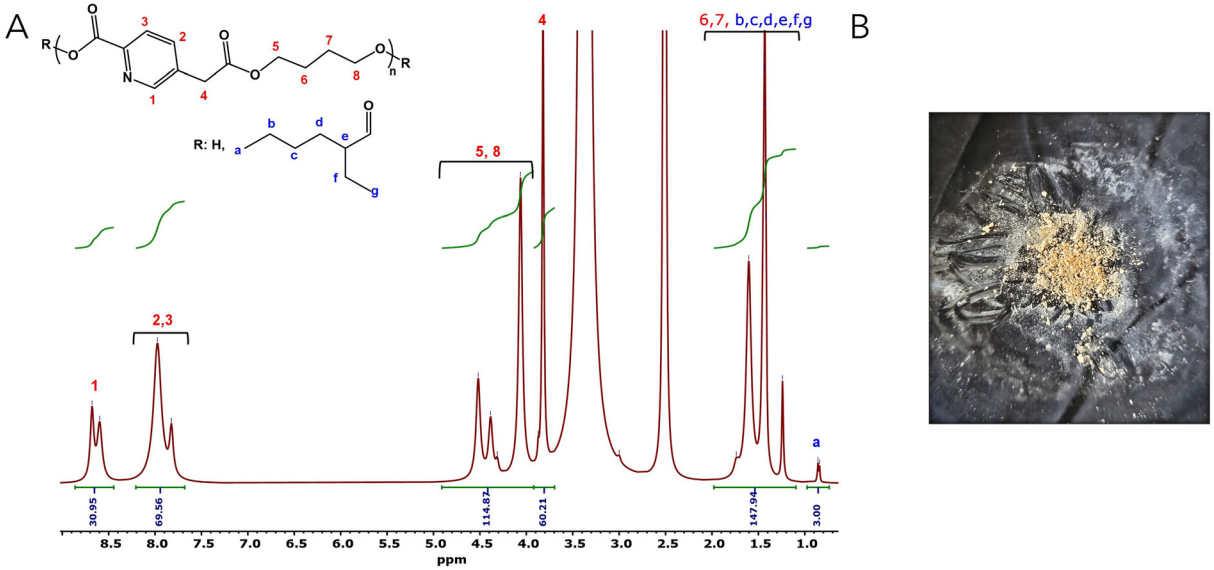

Fig. 5 PBCP synthesis. (A) Proton NMR spectrum of poly(1,4-butylene 5-(carboxymethyl)pyridine-2-carboxylate) (PBCP). Protons corresponding to the catalyst (a–g) are indicated in blue. Protons corresponding to the PBCP polymer (1–8) are indicated in red. Green lines represent the integration of the signals. (B) Photograph of the obtained polymer powder.

According to the NMR signals of the catalyst and the polymer, the value of the polymerization degree (n) is around 30. Thus, considering that the molecular weight of the repeating unit is 251 Da, PBCP has a satisfactory molecular weight of around 7300 Da. In addition, the ratio between 2,5-CPDCA and 1,4-butanediol can also be determined by NMR, which is near 50/50.

On the other hand, the average molecular weight determined by size exclusion chromatography (SEC) was 3300 Da with a dispersity ($Đ$) of 1.1, which indicates that the macromolecular growth was somehow controlled, and all the chains grew at a similar rate (Fig. S4). The lower molecular weight value of the polymer determined by SEC analysis is likely due to the fact that the molecular size standards used in SEC have a different structure and hydrodynamic ratio from the polymer synthesized in this work, hence suggesting that the molecular weight determined through end-group NMR analysis is the most accurate.

Poly(1,4-butylene 2,4-pyridinedicarboxylate) was enzymatically synthesized at low temperatures, obtaining molecular weights of around 1000–1400 Da.[38,75] The polyester presents semicrystalline behavior with melting temperatures of 104 °C and 157 °C, depending on whether the polymer was synthesized in bulk or diphenyl ether. Although the thermal degradation was analyzed and started at almost 290 °C, the T_g was not determined.[38] In this study, the synthesized PBCP polyester underwent thermal characterization by differential scanning calorimetry (DSC), utilizing the second heating run for analysis. The glass transition temperature (T_g) was determined to be 40 °C (Fig. S5), a value consistent with previously reported polyesters incorporating pyridine units. T_g values for derivatives of 2,6-PDCA with 1,3-propane diol and polyethylene glycol were determined to reach 30 °C and −30 °C, respectively.[37] However, to the best of our knowledge, only poly(1,4-butane 2,6-pyridinedicarboxylate) was analyzed in terms of glass transition temperature (T_g), with a value of 55.8 °C.[76] Since only the intrinsic viscosity of this polymer was provided and not its molecular weight, it was difficult to establish a direct correlation without knowing the Mark–Houwink–Sakurada parameters. The thermal stability of PBCP was evaluated by thermogravimetric analysis (TGA) in a single step (Fig. S6). Initially, there is continuous water elimination, marking the onset of degradation at 265 °C and reaching the maximum of weight loss at 365 °C (T_{d50} of 329 °C). These values are similar to those previously reported for PDCA-based polyesters.[38] Interestingly, the poly(1,4-butane 2,6-pyridinedicarboxylate) polymer can be coordinated with silver and copper to obtain complex polymers with good antimicrobial activity.[76] Therefore, the new PBCP polymer synthesized here could be of great interest to develop potent antibiofilm materials when complexed with certain metals.

Conclusions

In this work, we present a biological conversion strategy for the valorization of an underexplored lignin-derived monomer, *i.e.*, HVA, enabling the production of a novel building block, 2,5-CPDCA, for the synthesis of a new polyester material (PBCP). This efficient bioconversion process expands the catalogue of biologically produced PDCA-derived building blocks, offering a sustainable alternative to conventional chemical synthesis routes, which are often inefficient and environmentally detrimental. We successfully engineered a synthetic metabolic

pathway in *P. putida* KT2440 to convert HVA into 2,5-CPDCA, thereby enhancing the strain's versatility for transforming lignin-derived substrates into value-added compounds. The bioconversion of HVA, either as a pure compound or within real lignin depolymerization mixtures, was further optimized by engineering a second-generation biocatalyst expressing a heterologous ALAS enzyme, boosting intracellular 5-ALA levels. As 5-ALA is a key precursor of the heme cofactor required by the HmvABC cytochrome P450 system, this enhancement addressed the main bottleneck of the bioconversion, *i.e.*, the *O*-demethylation of HVA to HPC. Additionally, our work reveals that *P. putida* KT2440 expressing *hemA* is a promising microbial platform for bioprocesses involving heme-dependent enzymes.

This study serves as a proof of concept for an integrated biorefinery approach, in which lignin is first subjected to physicochemical depolymerization, followed by the biological conversion of selected monomers into novel building blocks such as 2,5-CPDCA. Since the 2,5-CPDCA titer achieved to date remains insufficient for industrial application, scalable strategies such as fed-batch cultivation, cell immobilization, and substrate concentration optimization should be explored in future studies to enhance production levels. Although we have accomplished an initial assessment of the polymerization properties of 2,5-CPDCA, future research is also required to fully explore its potential in the synthesis of new materials, not only bio-based homopolymers but, more importantly, co-polymers with enhanced functional and mechanical properties.

Author contributions

E. D., C. d. C.-S., and G. D.-R. conceived the project and designed the experiments. P. E.-N., C. d. C.-S., and G. D.-R. performed the experiments leading to the results described in the article. D. A. and F. M. performed the lignin depolymerization and monomers quantification assays. M. F.-G. and A. M.-B. performed the 2,4-CPDCA polymerization assays and the characterization of the PBCP polymer. All the authors analyzed the data and participated in the discussions included in this study. E. D., C. d. C.-S., and G. D.-R. wrote the manuscript.

Conflicts of interest

The authors declare competing financial interest. P. E.-N., C. d. C.-S., G. D.-R., and E. D. have submitted a patent application that includes some bioprocesses and strains engineered for this work.

Data availability

All the generated data are available within this paper and its supplementary information (SI). Supplementary information is available. See DOI: https://doi.org/10.1039/d6gc00315j.

Acknowledgements

We wish to thank A. Valencia for technical assistance. This work was supported by grant PID2022-142540OB-I00 of the Spanish Ministry of Science, Innovation and Universities MICIU/AEI/10.13039/501100011033, by grant CSIC 2024 20E138, and by the RELAY project supported by a fellowship from the Fundación General CSIC's ComFuturo program which has received funding from the European Union's Horizon 2020 research and innovation program under the Marie Skłodowska-Curie grant agreement No. 101034263.

References

1 D. S. Bajwa, G. Pourhashem, A. H. Ullah and S. G. Bajwa, *Ind. Crops Prod.*, 2019, **139**, 111526.
2 N. Li, S. Y. Zhu, L. L. Bai, B. Z. Li and Z. H. Liu, *Biotechnol. Adv.*, 2025, **83**, 108634.
3 X. L. Zhang, Z. H. Liu, B. Z. Li and Y. J. Yuan, *Green Chem.*, 2024, **26**, 11378–11405.
4 A. Liu, D. Ellis, A. Mhatre, S. Brahmankar, J. Seto, D. R. Nielsen and A. M. Varman, *Curr. Opin. Biotechnol.*, 2024, **89**, 103178.
5 N. Fu, R. Y. Liu, Y. Zhou, B. Z. Li, Y. J. Yuan and Z. H. Liu, *Green Chem.*, 2025, **27**, 4016–4039.
6 F. Weiland, M. Kohlstedt and C. Wittmann, *Metab. Eng.*, 2022, **71**, 13–41.
7 V. Sodré and T. D. H. Bugg, *Chem. Commun.*, 2024, **60**, 14360–14375.
8 M. E. Wolf and L. D. Eltis, *Trends Biochem. Sci.*, 2025, **50**, 322–331.
9 M. A. Pereyra-Camacho and I. Pardo, *Microb. Biotechnol.*, 2024, **17**, e14459.
10 D. Salvachúa, T. Rydzak, R. Auwae, A. De Capite, B. A. Black, J. T. Bouvier, N. S. Cleveland, J. R. Elmore, A. Furches, J. D. Huenemann, R. Katahira, W. E. Michener, D. J. Peterson, H. Rohrer, D. R. Vardon, G. T. Beckham and A. M. Guss, *Microb. Biotechnol.*, 2020, **13**, 290–298.
11 M. T. Manoli, Á. Gargantilla-Becerra, C. Del Cerro Sánchez, V. Rivero-Buceta, M. A. Prieto and J. Nogales, *Cell Rep.*, 2024, **43**, 113979.
12 H. Y. Jia, T. Xu, C. Wang, H. Zhu, B. Z. Li, Y. J. Yuan and Z. H. Liu, *Bioresour. Technol.*, 2025, **424**, 132278.
13 C. T. Palumbo, N. X. Gu, A. C. Bleem, K. P. Sullivan, R. Katahira, L. M. Stanley, J. K. Kenny, M. A. Ingraham, K. J. Ramirez, S. J. Haugen, C. R. Amendola, S. S. Stahl and G. T. Beckham, *Nat. Commun.*, 2024, **15**, 862.
14 C. R. Amendola, W. T. Cordell, C. M. Kneucker, C. J. Szostkiewicz, M. A. Ingraham, M. Monninger, R. Wilton, B. F. Pfleger, D. Salvachúa, C. W. Johnson and G. T. Beckham, *Metab. Eng.*, 2024, **81**, 88–99.
15 C. Liu, V. Juvonen, E. Meriläinen, E. Efimova, J. Luo, M. Salmela, S. Santala and V. Santala, *Microb. Cell Fact.*, 2025, **24**, 150.

16 M. Akutsu, N. Abe, C. Sakamoto, Y. Kurimoto, H. Sugita, M. Tanaka, Y. Higuchi, K. Sakamoto, N. Kamimura, H. Kurihara, E. Masai and T. Sonoki, *Bioresour. Technol.*, 2022, **359**, 127479.
17 F. Weiland, K. Seo, F. Janz, M. Grad, L. Geldmacher, M. Kohlstedt, J. Becker and C. Wittmann, *Metab. Eng.*, 2025, **92**, 262–283.
18 R. Y. Liu, C. Wang, B. Z. Li, Z. H. Liu and Y. J. Yuan, *Chem. Eng. J.*, 2024, **499**, 156286.
19 W. Niu, H. Willett, J. Mueller, X. He, L. Kramer, B. Ma and J. Guo, *Metab. Eng.*, 2020, **59**, 151–161.
20 Y. Higuchi, H. Ishimaru, T. Yoshikawa, T. Masuda, C. Sakamoto, N. Kamimura, E. Masai, D. Takeuchi and T. Sonoki, *Bioresour. Technol.*, 2023, **385**, 129450.
21 M. Kamada, C. Yasuta, Y. Higuchi, A. Yoshida, I. Kurnia, C. Sakamoto, A. Takeuchi, Y. Osaka, K. Muraki, N. Kamimura, E. Masai and T. Sonoki, *Microb. Cell Fact.*, 2024, **23**, 313.
22 H. Gómez-Álvarez, C. del Cerro-Sánchez, P. Iturbe, V. Rivero-Buceta, J. Nogales, T. D. H. Bugg and E. Díaz, *Green Chem.*, 2025, **27**, 3197–3206.
23 C. W. Johnson, D. Salvachúa, N. A. Rorrer, B. A. Black, D. R. Vardon, P. C. St John, N. S. Cleveland, G. Dominick, J. R. Elmore, N. Grundl, P. Khanna, C. R. Martinez, W. E. Michener, D. J. Peterson, K. J. Ramirez, P. Singh, T. A. Vander Wall, A. N. Wilson, X. Yi, M. J. Biddy and G. T. Beckham, *Joule*, 2019, **3**, 1523–1537.
24 R. Kato, E. Kuatsjah, M. Fujita, A. C. Bleem, S. Hishiyama, R. Katahira, T. Senda, G. T. Beckham, N. Kamimura and E. Masai, *Green Chem.*, 2025, **27**, 1540–1555.
25 B. Kim, J. M. Perez, S. D. Karlen, J. Coplien, J. T. Donohue and D. R. Noguera, *Green Chem.*, 2024, **26**, 7997–8009.
26 S. Notonier, A. Z. Werner, E. Kuatsjah, L. Dumalo, P. E. Abraham, E. A. Hatmaker, C. B. Hoyt, A. Amore, K. J. Ramirez, S. P. Woodworth, D. M. Klingeman, R. J. Giannone, A. M. Guss, R. L. Hettich, L. D. Eltis, C. W. Johnson and G. T. Beckham, *Metab. Eng.*, 2021, **65**, 111–122.
27 Z. Ookawa, Y. Higuchi, M. Fujita, T. Sonoki, N. Kamimura and E. Masai, *J. Agric. Food Chem.*, 2025, **73**, 18899–18913.
28 A. Z. Werner, W. T. Cordell, C. W. Lahive, B. C. Klein, C. A. Singer, E. C. D. Tan, M. A. Ingraham, K. J. Ramirez, D. H. Kim, J. N. Pedersen, C. W. Johnson, B. F. Pfleger, G. T. Beckham and D. Salvachúa, *Sci. Adv.*, 2023, **9**, eadj0053.
29 E. M. Spence, L. Calvo-Bado, P. Mines and T. D. H. Bugg, *Microb. Cell Fact.*, 2021, **20**, 1–12.
30 G. M. M. Rashid, V. Sodré, J. Luo and T. D. H. Bugg, *Biotechnol. Bioeng.*, 2024, **121**, 1366–1370.
31 H. Gómez-Álvarez, P. Iturbe, V. Rivero-Buceta, P. Mines, T. D. H. Bugg, J. Nogales and E. Díaz, *Bioresour. Technol.*, 2022, **346**, 126638.
32 J. Seeger, S. Müller, H. Gómez-Álvarez, G. M. M. Rashid, T. D. H. Bugg, E. Díaz and R. Takors, *Biotechnol. Bioeng.*, 2025, **122**, 2770–2780.
33 A. L. Yaguchi, S. J. Lee and M. A. Blenner, *Trends Biotechnol.*, 2021, **39**, 1037–1064.
34 E. M. Spence, H. T. Scott, L. Dumond, L. Calvo-Bado, S. di Monaco, J. J. Williamson, G. F. Persinoti, F. M. Squina and T. D. H. Bugg, *Appl. Environ. Microbiol.*, 2020, **86**, e01561–e01520.
35 D. J. Levy-Booth, M. M. Fetherolf, G. R. Stewart, J. Liu, L. D. Eltis and W. W. Mohn, *Front. Microbiol.*, 2019, **10**, 1862.
36 L. E. Navas, M. Zahn, H. Bajwa, J. C. Grigg, M. E. Wolf, A. C. K. Chan, M. E. P. Murphy, J. E. McGeehan and L. D. Eltis, *J. Biol. Chem.*, 2022, **298**, 101871.
37 S. Thiyagarajan, *Curr. Opin. Green Sustainable Chem.*, 2025, **53**, 101014.
38 A. Pellis, J. W. Comerford, S. Weinberger, G. M. Guebitz, J. H. Clark and T. J. Farmer, *Nat. Commun.*, 2019, **10**, 1762.
39 D. A. Holmer, *J. Polym. Sci., Part A-1*, 1968, **6**, 3177–3181.
40 O. B. Edgar and R. Hill, *J. Polym. Sci.*, 1952, **8**, 1–22.
41 J. Stouten, A. A. Wróblewska, G. Grit, J. Noordijk, B. Gebben, M. H. M. Meeusen-Wierts and K. V. Bernaerts, *Polym. Chem.*, 2021, **12**, 2379–2388.
42 R. I. Dowell and E. M. Hadley, *J. Med. Chem.*, 1992, **35**, 800–804.
43 D. Aboagye, F. Medina and S. Contreras, *Catal. Today*, 2023, **413**, 113969.
44 S. Totong, P. Daorattanachai, N. Laosiripojana and R. Idem, *Fuel Process. Technol.*, 2020, **198**, 106248.
45 N. Abad-Fernández, E. Pérez, A. Martín and M. J. Cocero, *J. Supercrit. Fluids*, 2020, **165**, 104940.
46 S. C. Patankar, L.-Y. Liu, L. Ji, S. Ayakar, V. Yadav and S. Renneckar, *Green Chem.*, 2019, **21**, 785–791.
47 L. Das and J. Shi, *Front. Energy Res.*, 2017, **5**, 21.
48 L. Li, S. Yu, C. Xie, F. Liu, S. Liu, K. Li and Z. Dong, *ACS Sustainable Chem. Eng.*, 2017, **5**, 382–391.
49 M. Kumar, S. You, J. Beiyuan, G. Luo, J. Gupta, S. Kumar, L. Singh, S. Zhang and D. C. W. Tsang, *Bioresour. Technol.*, 2021, **320**, 124412.
50 M. Bagdasarian, R. Lurz, B. Ruckert, F. C. Franklin, M. M. Bagdasarian, J. Frey and K. N. Timmis, *Gene*, 1981, **16**, 237–247.
51 E. Moreno-Ruiz, M. J. Hernáez, O. Martínez-Pérez and E. Santero, *J. Bacteriol.*, 2003, **185**, 2026–2030.
52 M. G. Acedos, I. de la Torre, V. E. Santos, F. García-Ochoa, J. L. García and B. Galán, *Biotechnol. Biofuels*, 2021, **14**, 8.
53 R. Silva-Rocha, E. Martínez-García, B. Calles, M. Chavarría, A. Arce-Rodríguez, A. de Las Heras, A. D. Páez-Espino, G. Durante-Rodríguez, J. Kim, P. I. Nikel, R. Platero and V. de Lorenzo, *Nucleic Acids Res.*, 2013, **41**, D666–D675.
54 J. Sambrook and D. W. Russel, in *Molecular cloning: a laboratory manual*, Cold Spring Harbor Laboratory Press, 3rd edn, 2001.
55 J. H. Miller, *Experiments in Molecular Genetics*, Cold Spring Harbor Laboratory, 1972.
56 M. J. López-Barragán, M. Carmona, M. T. Zamarro, B. Thiele, M. Boll, G. Fuchs, J. L. García and E. Díaz, *J. Bacteriol.*, 2004, **186**, 5762–5774.
57 R. Wirth, A. Friesenegger and S. Fiedler, *Mol. Gen. Genet.*, 1989, **216**, 175–177.

58 J. M. Klenk, M.-P. Fischer, P. Dubiel, M. Sharma, B. Rowlinson, G. Grogan and B. Hauer, *J. Biochem.*, 2019, **166**, 51–66.
59 D. I. Roper and R. A. Cooper, *FEBS Lett.*, 1990, **275**, 53–57.
60 Y. Honda, K. Nanasawa and H. Fujii, *ChemBioChem*, 2018, **19**, 2156–2159.
61 A. J. Fielding, J. D. Lipscomb and L. Que Jr, *J. Biol. Inorg. Chem.*, 2014, **19**, 491–504.
62 V. Méndez, L. Agulló, M. González and M. Seeger, *PLoS One*, 2011, **6**, e17583.
63 W. Guo, W. Zhou, H. Zhou and X. Chen, *BMC Microbiol.*, 2019, **19**, 1–11.
64 M. A. Prieto, E. Díaz and J. L. García, *J. Bacteriol.*, 1996, **178**, 111–120.
65 K. Adachi, Y. Takeda, S. Senoh and H. Kita, *Biochim. Biophys. Acta*, 1964, **93**, 483–493.
66 E. R. Blakley, H. Halvorson and W. Kurz, *Can. J. Microbiol.*, 1967, **13**, 159–165.
67 Y. Zhou, B. S. Sekar, S. Wu and Z. Li, *Biotechnol. Bioeng.*, 2020, **117**, 2340–2350.
68 J. C. Sadler and S. Wallace, *Green Chem.*, 2021, **23**, 4665–4672.
69 X. Wu, E. Smet, F. Brandi, D. Raikwar, Z. Zhang, B. U. W. Maes and B. F. Sels, *Angew. Chem., Int. Ed.*, 2024, **63**, e202317257.
70 K. Uchida, T. Akashi and T. Aoki, *Plant Biotechnol.*, 2015, **32**, 205–213.
71 H. Harada, K. Shindo, K. Iki, A. Teraoka, S. Okamoto, F. Yu, J. Hattan, R. Utsumi and N. Misawa, *Appl. Microbiol. Biotechnol.*, 2011, **90**, 467–476.
72 K. Sasaki, M. Watanabe, T. Tanaka and T. Tanaka, *Appl. Microbiol. Biotechnol.*, 2002, **58**, 23–29.
73 Y.-C. Yi, I.-T. Shih, T.-H. Yu, Y.-J. Lee and I.-S. Ng, *Bioresour. Bioprocess.*, 2021, **8**, 1–18.
74 S. J. Kwon, A. L. de Boer, R. Petri and C. Schmidt-Dannert, *Appl. Environ. Microbiol.*, 2003, **69**, 4875–4883.
75 J. W. Comerford, F. P. Byrne, S. Weinberger, T. J. Farmer, G. M. Guebitz, L. Gardossi and A. Pellis, *Materials*, 2020, **13**, 368.
76 S. Saleh, B. Sweileh, S. O. Taha, R. Mahmoud and M. O. Taha, *Molecules*, 2011, **16**, 933–950.